VSP

Advanced Composite Materials 17 (2008) 343–358

ADVANCED COMPOSITE MATERIALS
www.brill.nl/acm

A Study on Conceptual Structural Design of Wing for a Small Scale WIG Craft Using Carbon/Epoxy and Foam Sandwich Composite Structure

Changduk Kong [a,*], **Hyunbum Park** [a] **and Kukgin Kang** [b]

[a] Department of Aerospace Engineering, Chosun University, 375 Seosuk-dong Dong-gu, Gwangju 501-759, Republic of Korea

[b] WIG Research Center, Korea Ocean R&D Institute, 171 Jang-dong, Yuseong-gu, Daejeon 305-343, Republic of Korea

Received 3 August 2007; accepted 15 January 2008

Abstract

This present study provides the structural design and analysis of main wing, horizontal tail and control surface of a small scale WIG (Wing-in-Ground Effect) craft which has been developed as a future high speed maritime transportation system of Korea. Weight saving as well as structural stability could be achieved by using the skin–spar–foam sandwich and carbon/epoxy composite material. Through sequential design modifications and numerical structural analysis using commercial FEM code PATRAN/NASTRAN, the final design structural features to meet the final design goal such as the system target weight, structural safety and stability were obtained. In addition, joint structures such as insert bolts for joining the wing with the fuselage and lugs for joining the control surface to the wing were designed by considering easy assembling as well as more than 20 years service life.

Keywords

WIG (wing-in-ground effect) craft, structural design and analysis, carbon/epoxy, skin-spar-foam sandwich structure

1. Introduction

When a wing is flying close to the ground or on the water surface within a couple of meters height, the lift force is greatly increased due to the ground effect. Therefore, if a vehicle uses its wing with the ground effect, it is called a WIG (Wing-in-Ground Effect) craft. The WIG vehicle has a special feature that has a much wider wing than the conventional airplane wing and the hull type fuselage like a high speed boat. As a result, the WIG craft borrows some merits from both airplane and ship such that

* To whom correspondence should be addressed. E-mail: cdgong@mail.chosun.ac.kr

Edited by KSCM

DOI:10.1163/156855108X385302

it can transport quickly many passengers or heavy payload. Since the 1960s, many types of WIG crafts have been vigorously developed by Russia for military or civil uses [1, 2].

In Korea, vigorous study on the WIG craft has been progressing recently as a new generation maritime transportation system. For instance, KORDI (Korea Ocean Research and Development Institute) and some related industries have developed several classes of WIG crafts, such as those with 4 seats, 6 seats and 20 seats, a small scale WIG craft, and a 100 t large scale craft.

This study carried out a preliminary structural design and analysis on main wing, horizontal tail, control surface and joint parts of the 20-seat small scale WIG vehicle. The structural configuration adopted the skin–spar type structure with foam sandwich, and the main material was composed of carbon/epoxy composite. The initial design was performed using the netting rule and the rule of mixture. Structural safety and stability evaluation on the design features was done by a commercial FEM code NASTRAN. Through several modifications, the final structural design features were obtained to meet the design requirements of the system, namely, target weight, structural safety and stability.

2. Preliminary Structural Design

2.1. Design Outline

The structural design proof load of the main wing and horizontal tail was defined through the small scaled WIG vehicle's design requirements and load case analysis, and also the carbon/epoxy composite material was selected by reviewing how the mechanical properties of the selected composite material would react on the adopted structure [3].

The initial structural configuration adopted the skin–spar structural type, which is based on the defined proof load. The netting rule and the rule of mixture were used for initial structural designing. In order to confirm the structural safety of the initial structural design, structural analysis was performed by using FEM code. From the structural analysis on the first design configuration, some modifications were made because of a weak area on buckling and the design was somewhat heavier than the target weight.

The final structural configuration was fixed through several repeated design modifications and analyses. Figure 1 shows the 20-seat small scale WIG craft's aerodynamic configuration and the initial structural feature with the skin–spar type wing and tail.

2.2. Definition of Structural Design Load

The 20-seat small scale WIG craft's design requirements are a payload of 2 t, maximum cruising speed of 150 km/h in ground effect zone, maximum cruising speed of 170 km/h out of ground effect zone, a cruising altitude of 2 m, and a range of 1000 km. A modified NACA 7409 airfoil was adopted to improve the aerodynamic

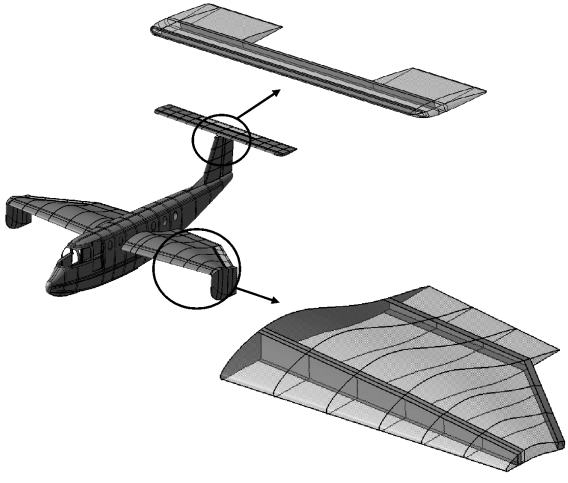

Figure 1. 3-D model for whole WIG craft, main wing and horizontal tail structure.

performance of the wing. The maximum lift coefficient is 0.73 at 4° (in ground effect). Chord lengths at wing root and tip are 7.5 m and 3.0 m, respectively, and half span is 9.0 m. The horizontal tail has a chord length of 2.3 m and span of 12.96 m. Target weights of the half span wing and the full span horizontal tail are 383 kg and 180 kg, respectively.

The structural design load of the main wing was defined from the relationship between the main wing's lift, the horizontal tail's lift and the inertia load at maximum cruising speed. The main wing load distribution was applied using the chordwise and spanwise distributed load equations [4] in considering the load factor of 2 that was given by the system design requirement. In this study, the main wing load was calculated with 20 segments divided spanwise by consideration of the inertia load due to dead weight [4]. The design proof load was defined as 1.5 times that of the calculated structural load. Because two engines are installed on the main wing by the engine mounting frame, the load due to propeller thrust was calculated using the relationship between brake horsepower and propeller efficiency. Figure 2 shows shear force and bending moment diagrams of the main wing.

The structural design load of the horizontal tail was calculated from the steady state maximum load through consideration of the checked maneuver acceleration load in symmetric pitching maneuver. The proof design load also was defined as 1.5 times the calculated horizontal tail's structural load, and the spanwise distributed loads were calculated using the same equation as that applied at the main wing. Figure 3 shows shear force and bending moment diagrams of horizontal tail.

2.3. Structural Design of Main Wing

The initial structural feature was a semi-monocoque type with skin and two spars for design simplification (see Fig. 1). It was initially composed of an 'I' type front spar and channel ('⊏') type rear spar including flange and web to avoid complex-

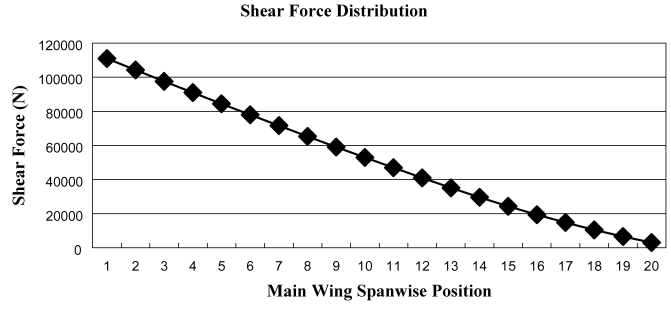

(a)

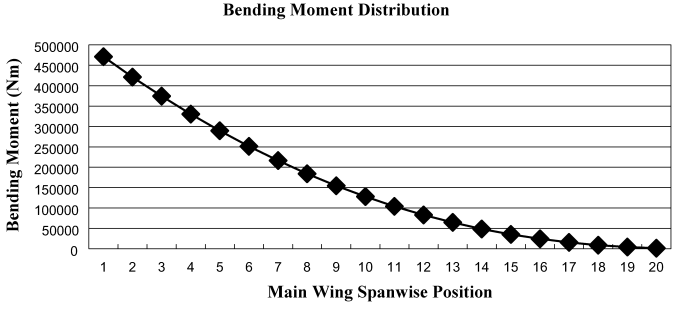

(b)

Figure 2. Shear force and bending moment diagram of main wing.

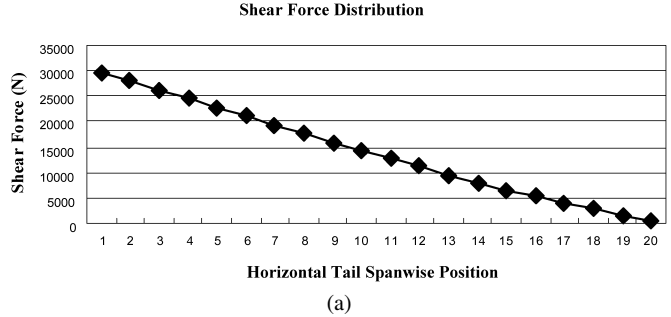

(a)

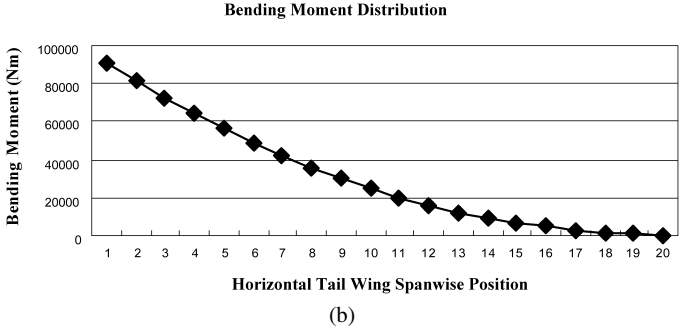

(b)

Figure 3. Shear force and bending moment diagram of horizontal tail.

ity of manufacturing of the selected carbon/epoxy composite laminate. Preliminary structural design was initially performed by the netting rule and the rule of mixture [5, 6]. According to the netting rule, the principal load directional thickness of the main spar flange and web can be sized by the crippling buckling strength 'σ_{crip}' as follows:

$$\left|\frac{F_x}{A} + \frac{M_z(\pm y)}{I_z}\right| \leqslant \left|\frac{X_{\text{t}}}{\text{S.F}}, \frac{\sigma_{\text{crip}}}{\text{S.F}}\right|, \tag{1}$$

$$\left|\frac{F_y}{A}\right| \leqslant \left|\frac{X_t}{\text{S.F}}, \frac{\sigma_{\text{crip}}}{\text{S.F}}\right|, \tag{2}$$

where F_x = spanwise load, F_y = chordwise load, A = flange's cross-sectional area, M_z = bending moment, X_{t} = fiber directional tensile strength, σ_{crip} = crippling buckling strength, I_z = area moment of inertia, and S.F = safety factor (fixed as 1.5).

However, the rule of mixture can consider approximately 10% additional load in off-loading directions at other inclined fiber directional plies. Therefore, the initially sized 0° ply flange thickness by the netting rule was modified by the rule of mixture with the added ±45° and 90° plies. The initial structural design results are shown in Table 1.

Table 1.
The initial structural design results of main wing

*Station	Front spar flange thickness (mm)	Stacking sequence
1	7.00	[2(±45, 0_4, 90, ±45, 0_4, 90)] s
2	5.25	[±45, 0_4, 90, ±45, 0_4, 90, ±45, 0_4, 90] s
3	2.75	[±45, 90, 0_4, ±45, 90, 0] s
4	1.75	[±45, 0_4, 90] s
5	1.25	[±45, 0_2, 90] s
6	1.25	[±45, 0_2, 90] s
	Rear spar flange thickness (mm)	
1	11.50	[2(±45, 90, 0_4, ±45, 90, 0_4, ±45, 90, 0_4, ±45)] s
2	7.75	[2(±45, 90, 0_4, ±45, 90, 0_4), ±45, 90] s
3	5.25	[±45, 0_4, 90, ±45, 0_4, 90, ±45, 0_4, 90] s
4	3.50	[±45, 0_4, 90, ±45, 0_4, 90] s
5	1.25	[±45, 0_2, 90] s
6	1.25	[±45, 0_2, 90] s
	Spar web thickness (mm)	
All	4.00	[2(±45, 0, 90, ±45, 0, 90)] s

Front and rear spar flange width: 225 mm.
* Where stations are defined in Fig. 1.

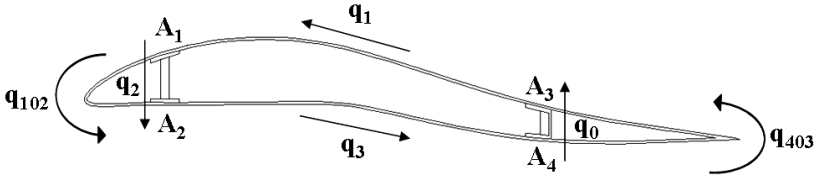

Figure 4. Shear flow of skin and spar web.

Skin thickness can be sized by the following equation by consideration of shear flows q_i of skin and web:

$$q_i = \frac{Q_y I_z - Q_z I_{yz}}{I_y \cdot I_z - I_{yz}^2} \sum A_i y_i - \frac{Q_z I_y - Q_y I_{yz}}{I_y \cdot I_z - I_{yz}^2} \sum A_i z_i + q_0, \tag{3}$$

$$\tau_{\text{allow}} = \frac{q_i}{t}, \tag{4}$$

where $q_i =$ shear flow, $Q_y = y$ axis component shear force, $Q_z = z$ axis component shear force, I_z, I_y and $I_{yz} =$ 2nd area moment of inertias in z, y, and y–z axes, $\sum A_i y_i =$ 1st area moment of inertia in y axis, $\sum A_i z_i =$ 1st area moment of inertia in z axis. Figure 4 shows the shear flow on skin and spar webs.

2.4. Structural Design of Horizontal Tail

The horizontal tail was designed by using a similar procedure as that used with the main wing. The structural feature was composed of an 'I' type front spar and channel type rear spar to accommodate easily the control surface, such as the elevator. Initial structural design was performed by the netting rule and the rule of mixture in the same way as the main wing design. Table 2 shows initial structural design results of the horizontal tail.

2.5. Evaluation of Structural Safety and Stability

In order to investigate structural safety and stability on the initially designed main wing and horizontal stabilizer, structural analysis was performed using the well-known commercial finite element code, PATRAN/NASTRAN. The element type used for this composite analysis was the laminated composite shell element 'PCOMP'.

Through stress analysis for structural safety using the Tsai-Wu failure criterion and structural stability analysis using the buckling load factor, it was found that the upper skin between the front spar and rear spars of the main wing was unstable in buckling at the given design load. Maximum stresses, of which maximum compressive stress is −67 MPa and maximum tensile stress is 65 MPa, were found around the joint part between wing and fuselage. The estimated weight of the initially designed wing was 395 kg, which is somewhat heavier than the target weight of 383 kg, and the wing tip deflection was 259 mm.

From stress analysis it was found that the initially designed horizontal tail was somewhat lighter than the target weight. However, the upper skin between the front

Table 2.
The initial structural design results of horizontal tail

Station	Front spar flange thickness (mm)	Stacking sequence
1	7.5	$[2(\pm 45, 90, 0_4, \pm 45, 90, 0_4), \pm 45]$ s
2	5	$[\pm 45, 0_4, 90, \pm 45, 0_4, 90, \pm 45, 0_3, 90]$ s
3	2.5	$[\pm 45, 0_3, 90, \pm 45, 0, 90]$ s
	Rear spar flange thickness (mm)	
1	5	$[\pm 45, 0_4, 90, \pm 45, 0_4, 90, \pm 45, 0_3, 90]$ s
2	2.5	$[\pm 45, 0_3, 90, \pm 45, 0, 90]$ s
3	2.5	$[\pm 45, 0_3, 90, \pm 45, 0, 90]$ s
	Spar web, skin thickness (mm)	
All	3	$[\pm 45, 0_3, 90, \pm 45, 0_3, 90]$ s

Front and rear spar flange width: 97 mm.

and rear spars of the horizontal tail was unstable in buckling. At the initially designed horizontal tail, the maximum compressive stress and maximum tensile stress were −128 MPa and 110 MPa, respectively.

Because not only did the initially designed main wing's weight exceed the target weight but also the upper skins of the main wing and horizontal tail were unstable in buckling, in order to meet the design requirements the specifications clearly needed to be modified.

3. Design Modifications

3.1. Design Modifications of Main Wing

In the first design modification, a middle spar was added between the front spar and the rear spar. Through buckling analysis, it was found that the upper skin between the middle and rear spars was unstable again even after the first design modification.

Therefore, in the second to the fourth design modifications, ribs were gradually added to remove the buckling. According to structural analysis results, because the first load factor of buckling was found to be 0.9, structural stability of the modified wing feature with ribs was obtained (Table 3). However the fourth modified wing feature's weight was 1.3 times that of the target weight.

For both weight reduction and structural stability, the skin-spar type feature with foam sandwich was finally adopted. According to structural analysis results for the final design feature, it was found that weight of the finally designed wing was slightly less than the target weight, and the structural safety was confirmed by safety factor evaluation using the Tsai-Wu failure criterion. In this calculation, it was found that the total weight of the main wing was 371.4 kg. As shown in Fig. 5,

Table 3.
Analysis result according to design modification of main wing

Design modification	Max stress (MPa)		First buckling load factor	Weight (kg)
	Comp.	Ten.		
Mod.1	−109	113	0.064	417.5
Mod.2	−105	107	0.9	497.3
Mod.3	−186	223	1.15	414.2
Mod.4	−120	114	2.78	371.4

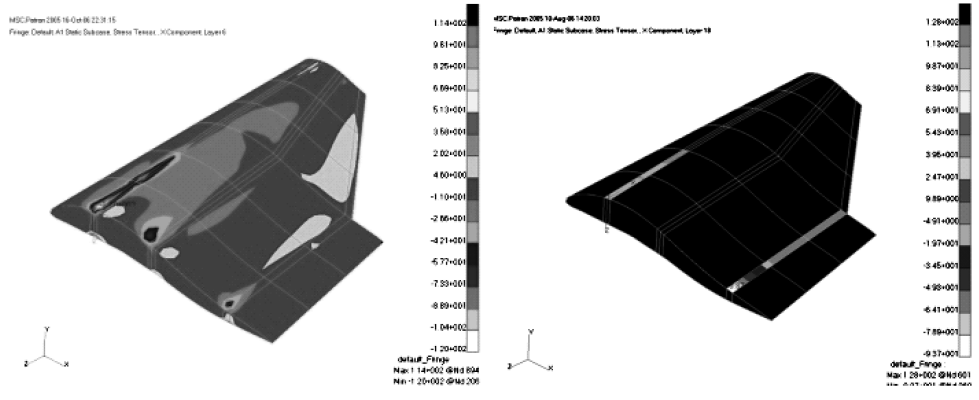

(a) (b)

Figure 5. Stress contour on skin and spar of final modified main wing.

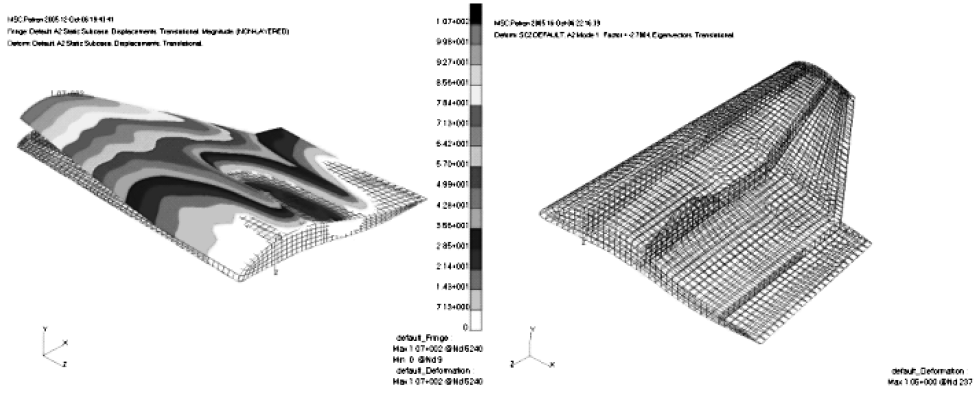

(a) (b)

Figure 6. Deformed configuration and first buckling mode shape of final modified main wing.

maximum compressive stress on the upper skin is −120 MPa, maximum tensile stress on the lower skin is 114 MPa. The first buckling load factor is 2.78. Figure 6

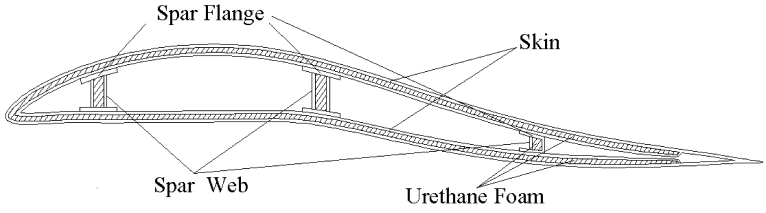

Figure 7. Final modification of main wing structure with three spars and foam sandwich.

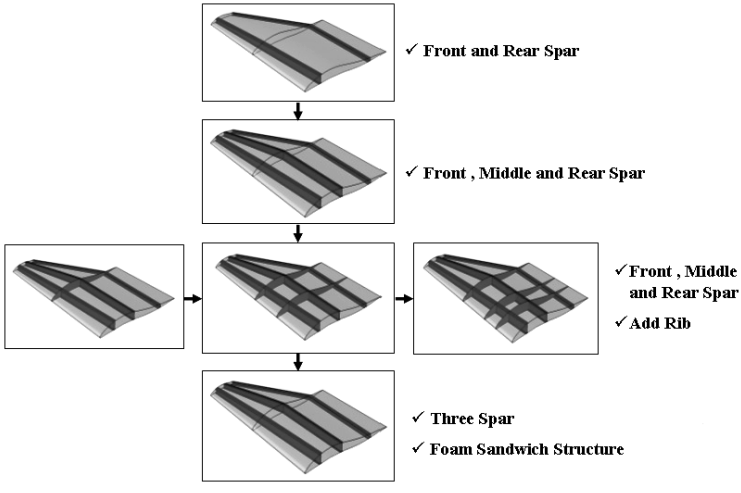

Figure 8. Design modification flow of main wing.

shows the deformed configuration and the first buckling mode shape of the finally modified main wing, and as shown in Fig. 7 the final modification feature of main wing is composed of three spars and skin with the foam sandwich. Figure 8 shows the design modification flow of main wing. Table 4 shows the sized thicknesses of spar flange, web and skin, and their laminate stacking sequences.

3.2. Design Modifications of Horizontal Tail

In the initial structural design and analysis, it was found that the upper skin between front and rear spars was unstable in bucking. In order to solve this buckling problem, the foam sandwich was added at upper skin and spar web as in the main wing design modification.

By stress analysis of the modified design feature, it was found that maximum compressive stress and tensile stress on the skin are −97.0 MPa and 97.1 MPa, respectively, compressive stress and tensile stress at the spar are −141 MPa and 101 MPa, respectively, and the structure is stable in bucking.

Figure 9 shows the stress contour on skin and spar of the modified horizontal tail, and Fig. 10 shows the deformed configuration and the first buckling mode shape. Table 5 shows final design modification results.

Table 4.
Final modification results of main wing structure

Station	Front spar flange thickness (mm)	
1	4.25	$[\pm 45, 0_4, 90, 0_4, \pm 45, 0_3, 90]$ s
2	3.75	$[\pm 45, 0_4, 90, \pm 45, 0_3, 90, \pm 45]$ s
3	2.00	$[\pm 45, 0_3, \pm 45, 0]$ s
4	1.75	$[\pm 45, 0_3, 90, 0]$ s
5	1.75	$[\pm 45, 0_3, 90, 0]$ s
6	1.75	$[\pm 45, 0_3, 90, 0]$ s
	Middle spar flange thickness (mm)	
All	2.00	$[\pm 45, 0_3, \pm 45, 0]$ s
	Rear spar flange thickness (mm)	
1	6.00	$[\pm 45, 90, 0_4, \pm 45, 90, 0_4, \pm 45, 0_4, \pm 45, 0_2]$ s
2	4.25	$[\pm 45, 0_4, 90, 0_4, \pm 45, 0_3, 90]$ s
3	3.75	$[\pm 45, 0_4, 90, \pm 45, 0_3, 90, \pm 45]$ s
4	2.00	$[\pm 45, 0_3, \pm 45, 0]$ s
5	1.75	$[\pm 45, 0_3, 90, 0]$ s
6	1.75	$[\pm 45, 0_3, 90, 0]$ s
	Spar web and skin thickness (mm)	
All	16.75	$[\pm 45, 0, 90, \pm 45, 0]$, foam, $[0, \pm 45, 90, 0, \pm 45]$

Front and rear spar flange width: 225 mm.
Foam sandwich thickness of web and skin: 15 mm.

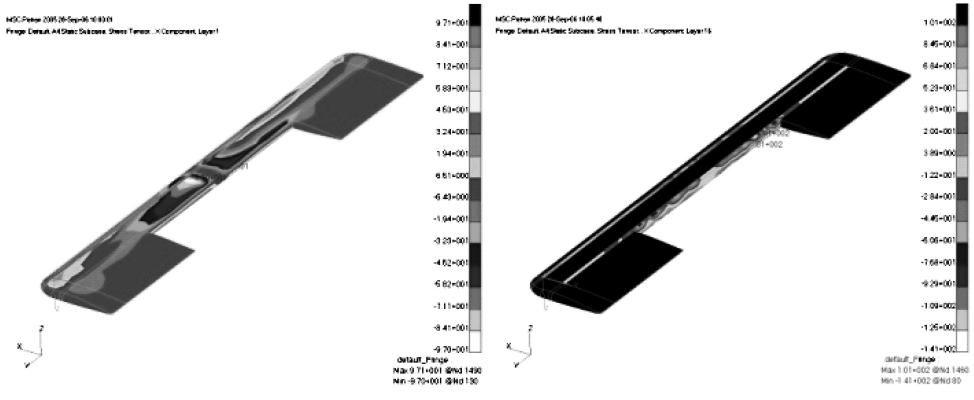

(a) (b)

Figure 9. Stress contour on skin and spar of the modified horizontal tail.

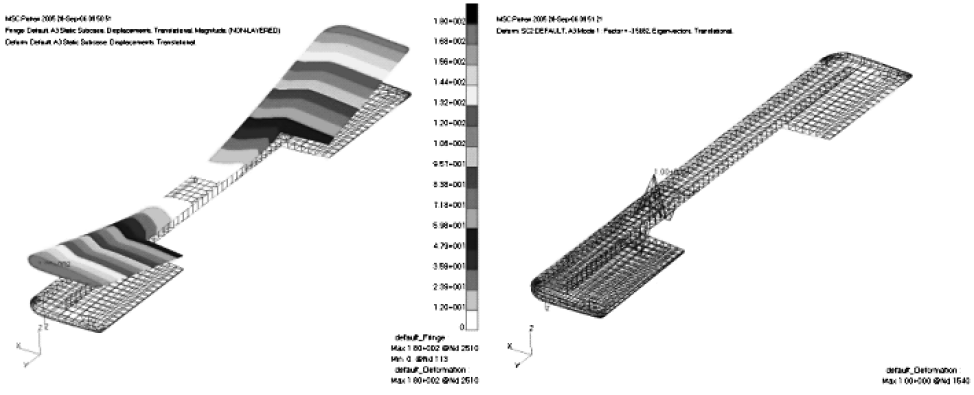

(a) (b)

Figure 10. Deformed configuration and the first buckling mode shape of the modified horizontal tail.

Table 5.
Final modification results of horizontal tail structure

Station	Front spar flange thickness (mm)	Stacking sequence
1	7.5	$[2(\pm 45, 90, 0_4, \pm 45, 90, 0_4), \pm 45]$ s
2	5	$[\pm 45, 0_4, 90, \pm 45, 0_4, 90, \pm 45, 0_3, 90]$ s
3	2.5	$[\pm 45, 0_3, 90, \pm 45, 0, 90]$ s
	Rear spar flange thickness (mm)	
1	5	$[\pm 45, 0_4, 90, \pm 45, 0_4, 90, \pm 45, 0_3, 90]$ s
2	2.5	$[\pm 45, 0_3, 90, \pm 45, 0, 90]$ s
3	2.5	$[\pm 45, 0_3, 90, \pm 45, 0, 90]$ s
	Spar web, skin thickness (mm)	
All	16.75	$(\pm 45, 0, 90, \pm 45, 0)$, foam, $(0, \pm 45, 90, 0, \pm 45)$

Front and rear spar flange width: 97 mm.
Foam sandwich thickness of web and skin: 15 mm.

4. Design on Joint Part and Control Surface

4.1. Joint Design Between Main Wing and Fuselage

For the wing root joint to fuselage, the insert type bolts were adopted through reinforcing root spar flanges. By considering principal stresses and allowable strength of the insert bolt, the titanium based steel alloy M30 bolt was selected for anti-corrosion against sea water environmental conditions.

In the first design, four bolts were applied to root flanges of the front and rear spars. The safety factor was calculated as 2.48 for the maximum static load in this case. By considering the dynamic load that may occur in flight and the fatigue limit

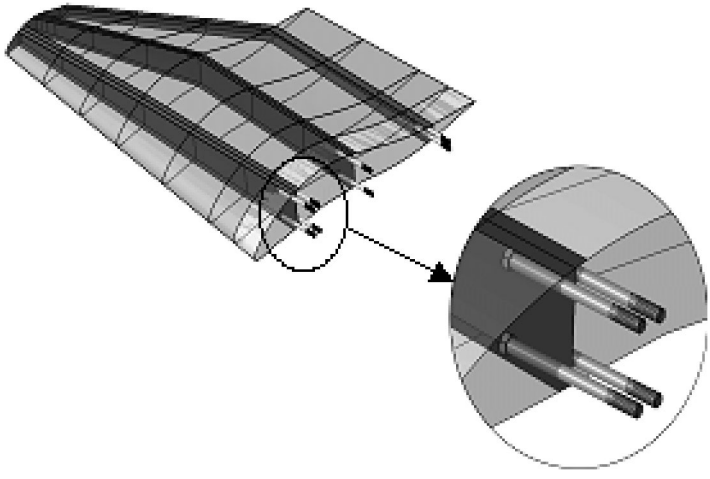

Figure 11. Joint part configuration of main wing.

load for more than 20 years fatigue life, 6 insert bolts comprising 4 bolts at the front root spar flange and 2 bolts at the rear root spar flange were decided on.

However, because the final design modification feature of main wing has 3 spars, 2 more bolts were added at the middle root spar flange. Therefore 8 insert bolts including 4 bolts at the front root spar flange and 2 bolts at the middle root spar flange and 2 bolts at the rear root spar flange were finally decided on [7]. Figure 11 shows the joint part configuration of the final design feature.

4.2. Control Surface Design

For structural design of the aileron and elevator, a method similar to that used with the main wing and horizontal tail design was used: for instance, the channel shape spar was selected for easy joint shape with the wing or the horizontal tail, and for calculating structural design load distribution the control surface was longitudinally divided into 20 sections. The initially designed laminate stacking sequences for the aileron skin and spar were $[\pm 45°, 0°, 90°]$ s, respectively. Through structural analysis, it was found that the spar was unsafe in strength and the upper skin was locally unstable in buckling. In order to modify the first design feature, some more plies of the spar flange were added, and the foam sandwich was added to the skin.

Therefore, the modified stacking sequence was $[\pm 45°, 0°, 90°, 0°, \pm 45°, 0°]$ s and the added foam thickness was 15 mm. In other words, the final laminate stacking sequence was decided as $[\pm 45°, 0°, 90°,$ foam, $90°, 0°, \pm 45°]$ s. According to stress analysis, it was found that not only was the final feature safe in strength because maximum compressive stress on the upper skin and maximum tensile stress on the lower skin were -52.8 MPa and 33.0 MPa, respectively, but also the structure was stable in buckling because the first buckling load factor was 1.03.

Two lugs which are located at $1/4$ position from the end of the control surface, respectively, were selected for the joint between the aileron and wing as shown in

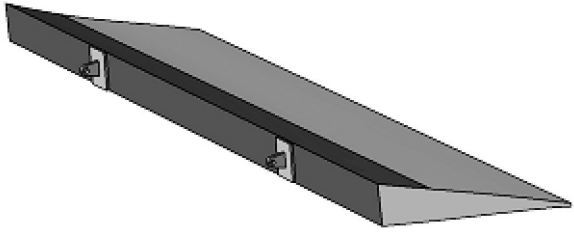

Figure 12. 3-D CATIA model for control surface.

Fig. 12. The lug design load was estimated from control surface movement in the slant direction, and aluminum alloy 7075-T6 material was selected for light weight.

The lug can be sized by the following equations (5) and (6) and the proper safety factor on the design load:

$$P_{\text{tru}} = K_{\text{tru}} f_{\text{tux}} \, \text{d}t, \tag{5}$$

$$\text{S.F} = \frac{P_{\text{tru}}}{P_{\text{a}}} > 1, \tag{6}$$

where P_{tru} = allowable critical load, K_{tru} = efficiency factor, F_{tux} = tensile strength of material, d = diameter of lug hole, t = lug thickness and P_{a} = applied load on control surface.

5. Structural Test

Before manufacturing the full scale WIG prototype, in order to evaluate structural design and analysis procedure the structural test was performed on a sub-scale main wing with the scaling ratio of 1/17. The subscale wing configuration is slightly different form the full scale one due to the manufacturing difficulties and the laboratory autoclave size. The sub-scale static structural test was performed under the simulated aerodynamic loads at three positions. The manufactured carbon/epoxy composite wing was set on the test rig and loaded by three steel weights. Figure 13 shows the experimental test setup of the sub-scale wing. Table 6 shows comparison results between the measured value and the predicted value on the stresses at the 10.4 mm region from wing root.

In order to find the natural frequency of the sub-scale wing, an experimental test was carried out using an impulse hammer, and the natural frequencies were found by the FFT analyzer. Table 7 shows the measured and predicted first mode natural frequencies.

In this comparison, it was inferred that the differences between the test results and the predicted values are caused by an incorrect test specimen that resulted from a rather excessive coating and adhesive treatment.

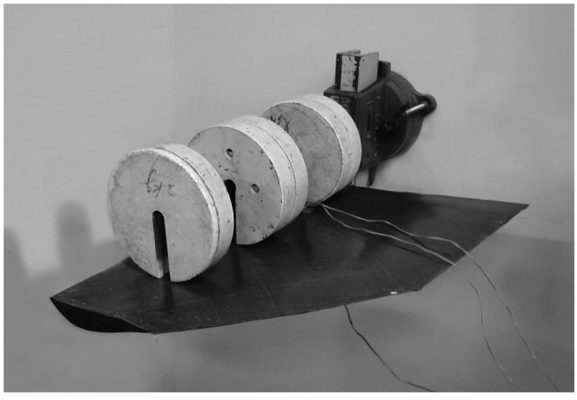

Figure 13. Static structural test setup of the sub-scale wing loaded by the simulated aerodynamic load with three steel weights.

Table 6.
Comparison between the tested and predicted stress results

Item	Analysis results	Test results
Upper surface stress	−20.7 MPa	−17.2 MPa
Lower surface stress	+6.81 MPa	+5.32 MPa

Table 7.
Comparison between the measured and predicted natural frequencies

Item	Analysis results	Test results
First flap mode	5.53 Hz	4.12 Hz

6. Fatigue Life Estimation

The fatigue life of the final design feature was estimated using the S–N diagram based on the reference carbon/epoxy materials, and confirmed the required system fatigue life of 20 years (Fig. 14). If a safety factor of 3 may be considered reasonable, then the WIG craft will operate with the following assumptions: 12 flights of 1 h duration each day, giving a total number of flights during 20 years of service as 87,699 times. If the safety factor of 3 may be considered as acceptable, the total number of flights can be modified to 262,800 times.

Because the weakest area for the fatigue during operation was found on the wing attachment ring frame, and the stress ratio with the maximum compressive stress of −120 MPa was 17, the fatigue life of the given composite material is about $N = 10^6$ cycles at 120 MPa if it may be assumed that the fatigue strength was reduced by

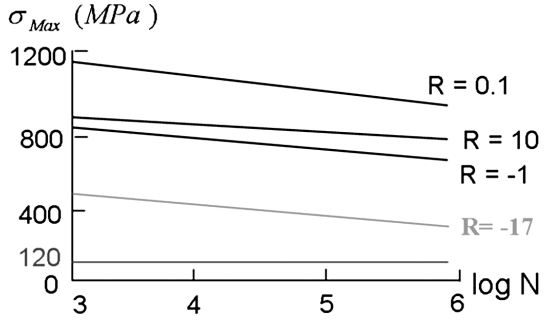

Figure 14. S–N curves of carbon/epoxy material (UD).

85% due to operation in sea water environment. Therefore the required mission fatigue cycle for 20 years operation is less than the given material fatigue life at the same stress level, the designed structure may be safe for the required fatigue life.

7. Conclusion

In this study, a structural conceptual design and analysis for the wing and horizontal tail of a 20-seat small scale WIG craft considering weight minimization was performed. The basic structural feature adopted the skin–spar type structure, and especially the foam sandwich composite was applied on the upper and lower surfaces of the wing to improve buckling behavior and vibration absorption capability. The front spar adopted an 'I' type beam and the rear spar adopted a channel type beam to accommodate control surface structure. In order to improve the strength to weight ratio as well as stiffness to weight ratio, the carbon/epoxy composite material which is mostly used in aerospace vehicle design was selected.

Through investigation of various load cases, the aerodynamic load including inertia load at the maximum cruising speed was defined as a structural design load. For light structural design concept, the carbon/epoxy composite material was selected, and for initial structural design of the spar flange and web of main wing and horizontal stabilizer the netting rule and the rule of mixture design methods were used. In this design, it was assumed that front and rear spar flanges endure mainly bending load, and skin and the spar webs endure the shear load. Through FEM analysis for evaluating structural safety and stability, several cycles of structural modifications were repeatedly carried out to meet the given target weight of 383 kg.

From structural stability analysis results of the initially designed main wing, it was found that the upper skin structure between front and rear spars was weak against buckling. Therefore in order to solve this problem, a middle spar and the foam sandwich at the upper skin and the web were added. After several design modifications, the structural safety and stability of the final design feature were reconfirmed. An insert bolt type wing joint structure with eight high-strength bolts to fix the designed wing to fuselage was adopted for easy assembly and removal as

well as in consideration of more than 20 years fatigue life. The final wing design feature's weight was 371.4 kg, which is 11.6 kg less than the target weight.

The horizontal stabilizer was designed using a similar structural feature to that used with the main wing. From buckling analysis of the initially designed horizontal stabilizer, it was found that the upper skin was somewhat weak against buckling, like the initially designed wing. Therefore the foam sandwich structure was added at the upper skin and spar web. Structural safety and stability of the final design feature was reconfirmed from the FEM analysis. The final horizontal tail design feature's weight was 150 kg which is 30 kg less than the target weight.

The structural design of the control surface including joint structure between main wing and control surface was performed. A structural feature with a channel type spar, the foam sandwich–carbon/epoxy composite skin structure and two lug joints was adopted for aileron design.

Before manufacturing the full scale WIG prototype, the structural test was performed by a sub-scale main wing for evaluation of the proposed structural design and analysis procedure. Through this comparison, even though there were some differences between them, it was confirm that the proposed design method is appropriate for the WIG's composite wing structure.

Acknowledgement

This study was supported by research funds from Chosun University, 2008.

References

1. N. Kornev and K. Matveev, Complex numerical modeling of dynamics and crashes of Wing-In-Ground vehicles, *AIAA*, 2003–600 (2003).
2. K. Benedict, N. Kornev, M. Meyer and J. Ebert, Complex mathematical model of the WIG motion including the take-off mode, *Ocean Engng* **29**, 315–357 (2002).
3. M. C. Y. Niu, *Composite Airframe Structure*. McGraw-Hill Book Company, New York, NY (1950).
4. F. Wojewodka, *Design of Simple Light Aircraft*. Cranfield University, UK (1973).
5. I. R. Farrow, *An Introduction to Composite Materials*. Department of Aerospace Engineering, Bristol, Lecture Note (1998).
6. E. F. Bruhn, *Analysis and Design of Flight Vehicle Structures*. Tri-State Offset Company, USA (1973).
7. C. Kong, Structural investigation of composite wind turbine blade considering various cases and fatigue life, *Energy* **30**, 2101–2114 (2005).